Exploiting Higher Kinematic Performance - Using a 4-Legged Redundant PM Rather than Gough-Stewart Platforms

Chapter · March 2012

DOI: 10.5772/32141 · Source: InTech

CITATIONS
10

READS
3,090

3 authors:

Mohammad H. Abedin-Nasab
Rowan University
38 PUBLICATIONS **242** CITATIONS
SEE PROFILE

Yong-jin Yoon
Korea Advanced Institute of Science and Technology
127 PUBLICATIONS **3,653** CITATIONS
SEE PROFILE

Hassan Zohoor
Sharif University of Technology
76 PUBLICATIONS **648** CITATIONS
SEE PROFILE

3

Exploiting Higher Kinematic Performance – Using a 4-Legged Redundant PM Rather than Gough-Stewart Platforms

Mohammad H. Abedinnasab[1], Yong-Jin Yoon[2] and Hassan Zohoor[3]
[1]*Door To Door Company, Sharif University of Technology*
[2]*Nanyang Technological University*
[3]*Sharif University of Technology,*
The Academy of Sciences of IR Iran
[1,3]*Iran*
[2]*Singapore*

1. Introduction

It is believed that Gough and Whitehall (1962) first introduced parallel robots with an application in tire-testing equipments, followed by Stewart (1965) , who designed a parallel mechanism to be used in a flight simulator. With ever-increasing demand on the robot's rigidity, redundant mechanisms, which are stiffer than their non-redundant counterparts, are attracting more attention.

Actuation redundancy eliminates singularity, and greatly improves dexterity and manipulability. Redundant actuation increases the dynamical capability of a PM by increasing the load-carrying capacity and acceleration of motion, optimizing the load distribution among the actuators and reducing the energy consumption of the drivers. Moreover, it enhances the transmission characteristics by increasing the homogeneity of the force transmission and the manipulator stiffness (Yi et al., 1989). From a kinematic viewpoint, redundant actuation eliminates singularities (Ropponen & Nakamura, 1990) which enlarge the usable workspace, as well. The kinematic analysis on general redundantly actuated parallel mechanisms was investigated by Müller (2005).

A number of redundantly full-actuated mechanisms have been proposed over the years and some of them which are more significant are listed in this section. The spatial octopod, which is a hexapod with 2 additional struts, is one of them (Tsai, 1999). A 5-DOF 3-legged mechanism was proposed by Lu et al. (2008), who studied its kinematics, statics, and workspace. Staicu (2009) introduced a new 3-DOF symmetric spherical 3-UPS/S parallel mechanism having three prismatic actuators. As another work of Lu et al. (2009), they introduced and used 2(SP+SPR+SPU) serial–parallel manipulators. Wang and Gosselin (2004) addressed an issue of singularity and designed three new types of kinematically redundant parallel mechanisms, including a new redundant 7-DOF Stewart platform. They concluded that such manipulators can be used to avoid singularities inside the workspace of non-redundant manipulators.

Choi et al. (2010) developed a new 4-DOF parallel mechanism with three translational and one rotational movements and found this mechanism to be ideal for high-speed machining.

Gao et al. (2010) proposed a novel 3DOF parallel manipulator and they increased the stiffness of their system, using an optimization technique. Lopes (2010) introduced a new 6-DOF moving base platform, which is capable of being used in micro robotic applications after processing serial combination with another industrial manipulator. It is in fact a non-redundant parallel mechanism with 6 linear actuators.
Deidda et al. (2010) presented a 3-DOF 3-leeged spherical robotic wrist. They analyzed mobility and singularity. Tale Masouleh et al. (2011) investigated the kinematic problem of a 5-DOF 5-RPUR mechanism with two different approaches, which differ by their concepts of eliminating passive variables. Zhao and Gao (2010) investigated the kinematic and dynamic properties of a 6-DOF 8-PSS redundant manipulator. They presented a series of new joint-capability indices, which are general and can be used for other types of parallel manipulators.
Li et al. (2007) worked on the singularity-free workspace analysis of the general Gough–Stewart platform. In a similar line of work, Jiang and Gosselin (Jiang & Gosselin, 2009a;b;c) determined the maximal singularity-free orientation workspace at a prescribed position of the Gough–Stewart platform. Alp and Ozkol (2008) described how to extend the workspace of the 6-3 and 6-4 Stewart platforms in a chosen direction by finding the optimal combination of leg lengths and joint angles. They showed that the workspace of the 6-3 Stewart platform is smaller than that of the 6-4 one.
Mayer and Gosselin (2000) developed a mathematical technique to analytically derive the singularity loci of the Gough-Stewart platform. Their method is based on deriving an explicit expression for the determinant of the jacobian matrix of the manipulator.
To demonstrate the redundancy effects, Wu et al. (2010) compared a planar 2-DOF redundant mechanism with its non-redundant counterpart. Arata et al. (2011) proposed a new 3-DOF redundant parallel mechanism entitled as Delta-R, based on its famous non-redundant counterpart, Delta, which was developed by Vischer & Clavel (1998).
Sadjadian and Taghirad (2006) compared a 3-DOF redundant mechanism, hydraulic shoulder, to its non-redundant counterpart. They concluded that the actuator redundancy in the mechanism is the major element to improve the Cartesian stiffness and hence the dexterity of the hydraulic shoulder. They also found that losing one limb reduces the stiffness of the manipulator significantly.
The rest of the chapter is organized as follows. In Section 2, in addition to introduction and comparison of non-redundant 3-legged and redundant 4-legged UPS PMs, four different architectures of the Gough-Stewart platforms are depicted. The kinematics of the abovementioned mechanisms are reviewed in Section 3. The jacobian matrices using the screw theory is derived in Section 4. In Sections 5 and 6, the performances of the redundant and non-redundant mechanisms are studied and compared with four well-known architectures of hexapods. Finally we conclude in Section 7.

2. Mechanisms description

The schematics of the 6-DOF non-redundant,3-legged and redundant 4-legged mechanisms are shown in Figs. 1 and 2, respectively.
The non-redundant 3-legged mechanism was first introduced by Beji & Pascal (1999). The redundant 4-legged mechanism has the similar structure, with a single leg added to the 3-legged system, which keeps symmetry. Each leg is composed of three joints; universal,

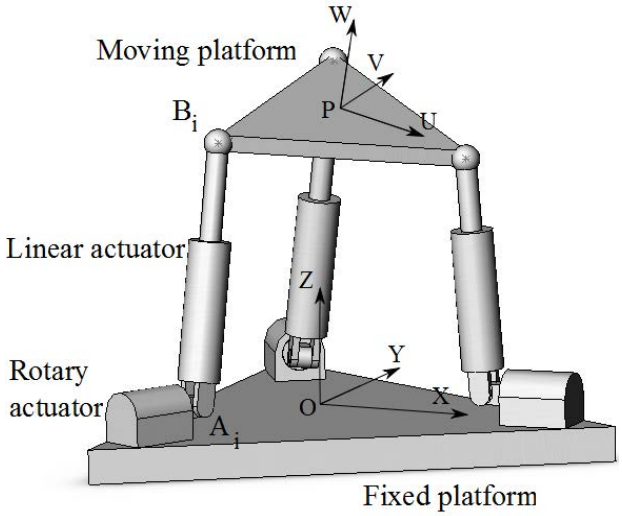

Fig. 1. Schematic of the non-redundant mechanism.

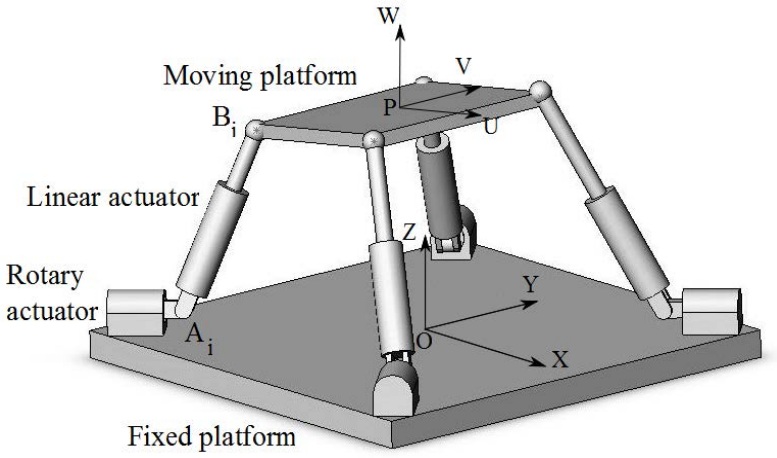

Fig. 2. Schematic of the redundant mechanism.

prismatic, and spherical (Fig. 3). A rotary actuator and a linear actuator are used to actuate each leg. The rotary actuators, whose shafts are attached to the lower parts of the linear actuators through the universal joints, are placed on the corners of the fixed platform (Abedinnasab & Vossoughi, 2009; Aghababai, 2005). The spherical joints connect the upper parts of the linear actuators to the moving platform.

Rotary actuators are situated on the corners A_i (for $i=1, 2, 3, 4$) of the base platform and each shaft is connected to the lower part of linear actuators through a universal joint (Figs. 1 and 2). The upper parts of linear actuators are connected to the corners of the moving platform, B_i points, through spherical joints (Fig. 3).

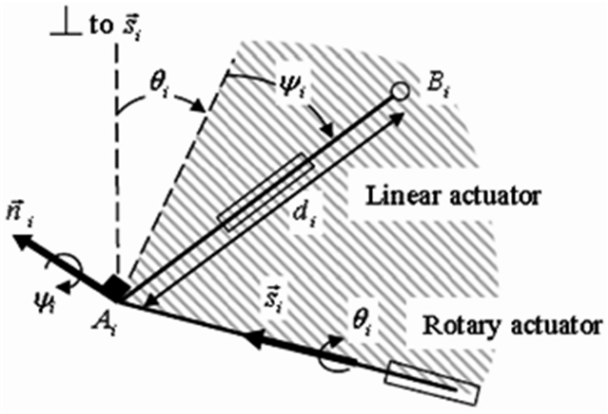

Fig. 3. Schematic of the universal joint, and the joints variables.

Cartesian coordinates A (O, x ,y, z) and B (P, u, v, w) represented by {A} and {B} are connected to the base and moving platforms, respectively. In Fig.3, $\vec{s}_i$ represents the unit vector along the axes of ith rotary actuator and $\vec{d}_i$ is the vector along $\overrightarrow{A_iB_i}$ with the length of d_i. Assuming that each limb is connected to the fixed base by a universal joint, the orientation of ith limb with respect to the fixed base can be described by two Euler angles, rotation θ_i around the axis $\vec{s}_i$, followed by rotation ψ_i around $\vec{n}_i$, which is perpendicular to $\vec{d}_i$ and $\vec{s}_i$ (Fig. 3). It is to be noted that θ_i and d_i are active joints actuated by the rotary and linear actuators, respectively. However, ψ_i is inactive.

By replacing the passive universal joints in the Stewart mechanism with active joints in the above mentioned mechanisms, the number of legs could be reduced from 6 to 3 or 4. This

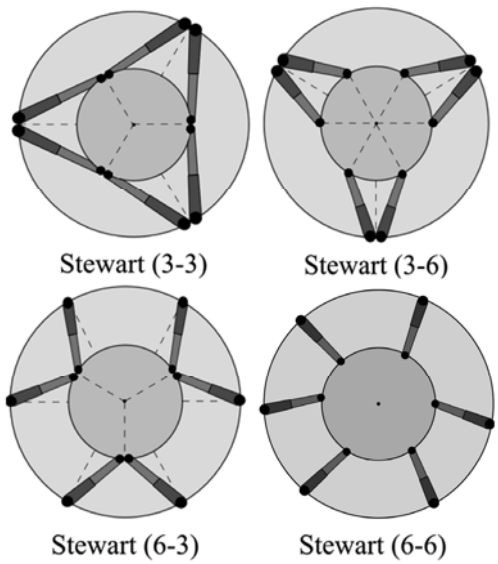

Fig. 4. Schematics of well-known Stewart platforms.

change makes the mechanism to be lighter, since the rotary actuators are resting on the fixed platform, which causes higher accelerations to be available due to smaller inertial effects.
The applications of this type of robots can be found in flight simulators, high precision surgical tools, positioning devices, motion generators, ultra-fast pick and place robots, haptic devices, entertainment, multi-axis machine tools, micro manipulators, rehabilitation devices, etc.
Advantages of high rigidity and low inertia make these PMs ideal for force feedback control, assembly, manufacturing, underground projects, space technologies, and biology projects.

3. Kinematic analysis

One of the most important issues in the study of parallel mechanisms is the kinematic analysis, where the generated results form the base for the application of the mechanism.
$\vec{a}_i$ represents the vector $\overrightarrow{OA_i}$ (Fig. 1). $\vec{a}_i = g[\cos\gamma_i \quad \sin\gamma_i \quad 0]^T$, in which,

$$\gamma_1^{Red.} = -45^\circ,\ \gamma_2^{Red.} = 45^\circ,\ \gamma_3^{Red.} = 135^\circ,\ and\ \ \gamma_4^{Red.} = -135^\circ,$$

and

$$\gamma_1^{Non-Red.} = 0^\circ,\ \gamma_2^{Non-Red.} = 120^\circ,\ and\ \ \gamma_3^{Non-Red.} = -120^\circ,$$

where g and r are the radius of the fixed and moving platforms, respectively. $\overrightarrow{{}^{B}b_i}$ represents the position of the ith joint on the platform in the moving frame {B}, $\overrightarrow{{}^{B}b_i} = \overrightarrow{PB_i}\Big)_B$. $\overrightarrow{{}^{B}b_i}$ is constant and is equal to $\overrightarrow{{}^{B}b_i} = h[\cos\gamma_i \quad \sin\gamma_i \quad 0]^T$. We can represent ${}^{A}_{B}R = \left[r_{ij} \right]$, the rotation matrix from $\{B\}$ to $\{A\}$, using Euler angles as

$${}^{A}_{B}R = \begin{bmatrix} c\alpha_2 c\alpha_3 & c\alpha_3 s\alpha_2 s\alpha_1 - s\alpha_3 c\alpha_1 & c\alpha_3 s\alpha_2 c\alpha_1 + s\alpha_3 s\alpha_1 \\ c\alpha_2 s\alpha_3 & s\alpha_3 s\alpha_2 s\alpha_1 + c\alpha_3 c\alpha_1 & s\alpha_3 s\alpha_2 c\alpha_1 - c\alpha_3 s\alpha_1 \\ -s\alpha_2 & c\alpha_2 s\alpha_1 & c\alpha_2 c\alpha_1 \end{bmatrix}, \tag{1}$$

where $s\alpha_1 = \sin\alpha_1$ and $c\alpha_1 = \cos\alpha_1$, and so on. α_1, α_2, and α_3 are three Euler angles defined according to the $z-y-x$ convention. Thus, the vector $\overrightarrow{{}^{B}b_i}$ would be expressed in the fixed frame {A} as

$$\vec{b}_i = {}^{A}_{B}R\,\overrightarrow{PB_i}\Big)_B. \tag{2}$$

Let $\vec{p}$ and $\vec{r}_i$ denote the position vectors for P and B_i in the reference frame $\{A\}$, respectively. From the geometry, it is obvious that

$$\vec{r}_i = \vec{p} + \vec{b}_i. \tag{3}$$

Subtracting vector $\vec{a}_i$ from both sides of (3) one obtains

$$\vec{r}_i - \vec{a}_i = \vec{p} + \vec{b}_i - \vec{a}_i. \tag{4}$$

Left hand side of (4) is the definition of $\overrightarrow{d_i}$, therefore

$$d_i^2 = (\vec{p} + \vec{b}_i - \vec{a}_i) \cdot (\vec{p} + \vec{b}_i - \vec{a}_i) . \tag{5}$$

Using Euclidean norm, d_i can be expressed as:

$$d_i = \sqrt{\left((x - x_i)^2 + (y - y_i)^2 + (z - z_i)^2\right)} , \tag{6}$$

where,

$$\begin{cases} x_i = -h\left(\cos\gamma_i r_{11} + \sin\gamma_i r_{21}\right) + g\cos\gamma_i \\ y_i = -h\left(\cos\gamma_i r_{12} + \sin\gamma_i r_{22}\right) + g\sin\gamma_i \\ z_i = -h\left(\cos\gamma_i r_{13} + \sin\gamma_i r_{23}\right) \end{cases} . \tag{7}$$

Coordinates $C_i(A_i, x_i, y_i, z_i)$ are connected to the base platform with their x_i axes aligned with the rotary actuators in the $\vec{s}_i$ directions, with their z_i axes perpendicular to the fixed platform. Thus, one can express vector $\overrightarrow{d_i}$ in $\{C_i\}$ as

$${}^{C_i}\overrightarrow{d_i} = d_i \begin{bmatrix} \sin\psi_i \\ -\sin\theta_i \cos\psi_i \\ \cos\theta_i \cos\psi_i \end{bmatrix} , \tag{8}$$

and from the geometry is clear that

$$\vec{r}_i = \vec{a}_i + {}^{A}_{C_i}R \, {}^{C_i}\overrightarrow{d_i} , \tag{9}$$

where ${}^{A}_{C_i}R$ is the rotation matrix from $\{C_i\}$ to $\{A\}$,

$${}^{A}_{C_i}R = \begin{bmatrix} \cos\gamma_i & -\sin\gamma_i & 0 \\ \sin\gamma_i & \cos\gamma_i & 0 \\ 0 & 0 & 1 \end{bmatrix} . \tag{10}$$

By equating the right sides of (3) and (4), and solving the obtained equation, ψ_i and θ_i can be calculated as follows:

$$\psi_i = \sin^{-1}\left(\frac{\cos\gamma_i (x - x_i) + \sin\gamma_i (y - y_i)}{d_i}\right) , \tag{11}$$

$$\theta_i = \sin^{-1}\left(\frac{\sin\gamma_i (x - x_i) - \cos\gamma_i (y - y_i)}{d_i \cos\psi_i}\right) . \tag{12}$$

4. Jacobian analysis using screw theory

Singularities of a PM pose substantially more complicated problems, compared to a serial manipulator. One of the first attempts to provide a general framework and classification may be traced back to Gosselin and Angeles (1990) ,who derived the input–output velocity map for a generic mechanism by differentiating the implicit equation relating the input and output configuration variables. In this way, distinct jacobian matrices are obtained for the inverse and the direct kinematics, and different roles played by the corresponding singularities are clearly shown.

For singularity analysis other methods rather than dealing with jacobian matrix are also available. Pendar et al. (2011) introduced a geometrical method, namely *constraint plane method*, where one can obtain the singular configurations in many parallel manipulators with their mathematical technique. Lu et al. (2010) proposed a novel analytic approach for determining the singularities of some 4-DOF parallel manipulators by using *translational/rotational jacobian matrices*. Piipponen (2009) studied kinematic singularities of planar mechanisms by means of *computational algebraic geometry* method. Zhao et al. (2005) have proposed *terminal constraint* method for analyzing the singularities based on the physical meaning of reciprocal screws.

Gosselin & Angeles (1990) have based their works on deriving the jacobian matrix. They performed this by defining three possible conditions. In these conditions the determinant of forward jacobian matrix or inverse jacobian matrix is investigated. They have shown that having dependent Plücker vectors in a parallel manipulator is equivalent to zero determinant of the forward jacobian matrix and then a platform singularity arises.

In this section the jacobian analysis of the proposed PMs are approached by using the theory of screws. Zhao et al. (2011) proposed a new approach using the screw theory for force analysis, and implemented it on a 3-DOF 3-RPS parallel mechanism. Gallardo-Alvarado et al. (2010) presented a new 5-DOF redundant parallel manipulator with two moving platforms, where the active limbs are attached to the fixed platform. They find the jacobian matrix by means of the screw theory.

A class of series-parallel manipulators known as 2(3-RPS) manipulators was studied by Gallardo-Alvarado et al. (2008) by means of the screw theory and the principle of virtual work. Gan et al. (2010) used the screw theory to obtain the kinematic solution of a new 6-DOF 3CCC parallel mechanism. Gallardo-Alvarado et al. (2006) analyzed singularity of a 4-DOF PM by means of the screw theory.

Hereafter we derive the jacobian matrices of the proposed mechanisms using screw theory. Joint velocity vector in the redundant mechanism, $\dot{\bar{q}}^{\mathrm{Red.}}$, is an 8×1 vector:

$$\dot{\bar{q}}^{\mathrm{Red.}} = [\ \dot{\theta}_1 \quad \dot{\theta}_2 \quad \dot{\theta}_3 \quad \dot{\theta}_4 \quad \dot{d}_1 \quad \dot{d}_2 \quad \dot{d}_3 \quad \dot{d}_4]^T \tag{13}$$

where $\dot{\theta}_i$ and $\dot{d}_i$ are the angular and linear velocities of the rotary and linear actuators, respectively. However, joint velocity vector in the non-redundant mechanism, $\dot{\bar{q}}^{Non-\mathrm{Red.}}$, is a 6×1 vector:

$$\dot{\bar{q}}^{Non-\mathrm{Red.}} = [\dot{\theta}_1 \quad \dot{\theta}_2 \quad \dot{\theta}_3 \quad \dot{d}_1 \quad \dot{d}_2 \quad \dot{d}_3]^T . \tag{14}$$

The linear and angular velocities of the moving platform are defined to be $\vec{v}$ and $\vec{\omega}$, respectively. Thus, $\dot{\vec{x}}$ can be written as a 6×1 velocity vector;

$$\dot{\vec{x}} = [\vec{v}^T \quad \vec{\omega}^T]. \tag{15}$$

Jacobian matrices relate $\dot{\vec{q}}$ and $\dot{\vec{x}}$ as follow;

$$J_x \dot{\vec{x}} = J_q \dot{\vec{q}}, \tag{16}$$

where J_x and J_q are forward and inverse jacobian matrices, respectively. If one defines J as follows;

$$J = J_q^{-1} J_x. \tag{17}$$

Thus $\dot{\vec{q}}$,and $\dot{\vec{x}}$ can be simply related as;

$$\dot{\vec{q}} = J\ \dot{\vec{x}}. \tag{18}$$

The concept of reciprocal screws is applied to derive J_x and J_q (Tsai, 1998; 1999). The reference frame of the screws is point P of the moving platform. Fig. 5 shows the kinematic chain of each leg, where universal joints are replaced by intersection of two unit screws, $\hat{\$}_1$ and $\hat{\$}_2$. $\hat{\$}_1 = \begin{bmatrix} \vec{s}_{1,i} \\ (\vec{b}_i - \vec{d}_i)\times \vec{s}_{1,i} \end{bmatrix}$ and $\hat{\$}_2 = \begin{bmatrix} \vec{s}_{2,i} \\ (\vec{b}_i - \vec{d}_i)_i \times \vec{s}_{2,i} \end{bmatrix}$ where $\vec{s}_{1,i}$ and $\vec{s}_{2,i}$ are unit vectors along the inactive and active joints of each universal joint, respectively. Spherical joints in each leg are replaced by intersection of three unit screws, $\hat{\$}_4$, $\hat{\$}_5$, and $\hat{\$}_6$. $\hat{\$}_4 = \begin{bmatrix} \vec{s}_{4,i} \\ \vec{b}_i \times \vec{s}_{4,i} \end{bmatrix}$, $\hat{\$}_5 = \begin{bmatrix} \vec{s}_{5,i} \\ \vec{b}_i \times \vec{s}_{5,i} \end{bmatrix}$, and $\hat{\$}_6 = \begin{bmatrix} \vec{s}_{6,i} \\ \vec{b}_i \times \vec{s}_{6,i} \end{bmatrix}$, where $\vec{s}_{4,i} = \vec{s}_{1,i}$, $\vec{s}_{6,i}$ is the unit vector along the linear actuator, and $\vec{s}_{5,i} = \vec{s}_{6,i} \times \vec{s}_{4,i}$. $\hat{\$}_3 = \begin{bmatrix} 0 \\ \vec{s}_{3,i} \end{bmatrix}$ explains the prismatic joint, as well. It is to be noted that $\vec{s}_{3,i} = \vec{s}_{6,i}$. Each leg can be assumed as an open-loop chain to express the instant twist of the moving platform by means of the joint screws:

$$\begin{aligned} \hat{\$}_P = {} & \dot{\psi}_i \hat{\$}_{1,i} + \dot{\theta}_i \hat{\$}_{2,i} + \dot{d}_i \hat{\$}_{3,i} + \dot{\phi}_{1,i} \hat{\$}_{4,i} \\ & + \dot{\phi}_{2,i} \hat{\$}_{5,i} + \dot{\phi}_{3,i} \hat{\$}_{6,i} \end{aligned}. \tag{19}$$

By taking the orthogonal product of both sides of (19) with reciprocal screw $\hat{\$}_{r1,i} = \begin{bmatrix} \vec{s}_{3,i} \\ \vec{b}_i \times \vec{s}_{3,i} \end{bmatrix}$, one can eliminate the inactive joints and rotary actuator which yields to

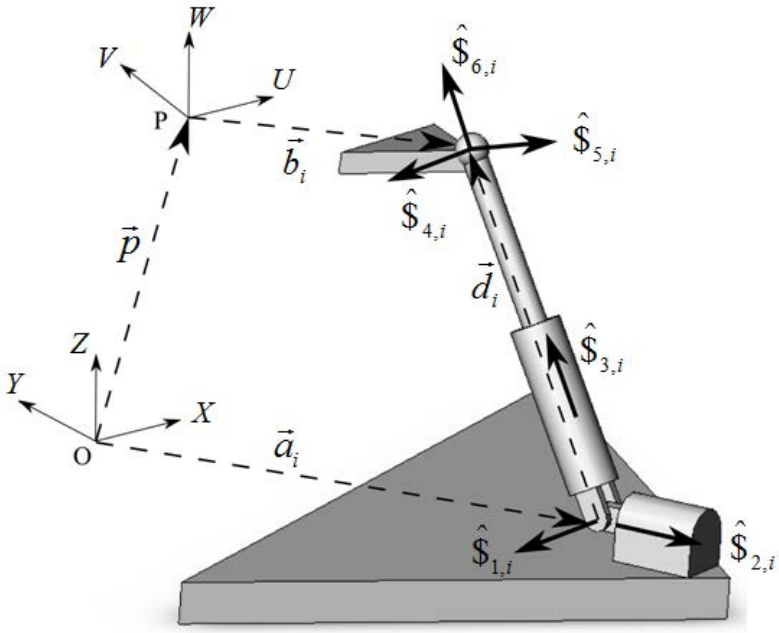

Fig. 5. Infinitesimal screws.

$$\left[\begin{array}{cc} \frac{\vec{d}_i^{\,T}}{d_i} & \frac{(\vec{b}_i \times \vec{d}_i)^T}{d_i} \end{array}\right] \dot{\vec{x}}_P = \dot{d}_i\,,\ i = 1,2,3,4\,. \tag{20}$$

Similarly, if one takes the orthogonal product of both sides of (19) with reciprocal screw $\hat{\$}_{r6,i} = \begin{bmatrix} \frac{\vec{s}_i \times \vec{d}_i}{d_i \cos\psi_i} \\ \vec{b}_i \times \frac{\vec{s}_i \times \vec{d}_i}{d_i \cos\psi_i} \end{bmatrix}$ the resultant is as follows;

$$\left[\begin{array}{cc} (\frac{\vec{s}_i \times \vec{d}_i}{d_i \cos\psi_i})^T & (\vec{b}_i \times \frac{\vec{s}_i \times \vec{d}_i}{d_i \cos\psi_i})^T \end{array}\right] \dot{\vec{x}}_P = d_i \cos\psi_i \dot{\theta}_i\,. \tag{21}$$

Note that in (21), $\left|\vec{s}_i \times \vec{d}_i\right| = d_i \cos\psi_i$.

Finally, using (20) and (21), jacobian matrices $J_x^{\mathrm{Red.}}$ and $J_q^{\mathrm{Red.}}$ are expressed as;

$$J_x^{\mathrm{Red.}} = \begin{bmatrix} (\vec{s}_1 \times \overrightarrow{d_1})^T & (\vec{b}_1 \times (\vec{s}_1 \times \overrightarrow{d_1}))^T \\ (\vec{s}_2 \times \overrightarrow{d_2})^T & (\vec{b}_2 \times (\vec{s}_2 \times \overrightarrow{d_2}))^T \\ (\vec{s}_3 \times \overrightarrow{d_3})^T & (\vec{b}_3 \times (\vec{s}_3 \times \overrightarrow{d_3}))^T \\ (\vec{s}_4 \times \overrightarrow{d_4})^T & (\vec{b}_4 \times (\vec{s}_4 \times \overrightarrow{d_4}))^T \\ \overrightarrow{d_1}^T & (\vec{b}_1 \times \overrightarrow{d_1})^T \\ \overrightarrow{d_2}^T & (\vec{b}_2 \times \overrightarrow{d_2})^T \\ \overrightarrow{d_3}^T & (\vec{b}_3 \times \overrightarrow{d_3})^T \\ \overrightarrow{d_4}^T & (\vec{b}_4 \times \overrightarrow{d_4})^T \end{bmatrix}, \tag{22}$$

and

$$J_q^{\mathrm{Red.}} = diag(d_1^2 \cos^2\psi_1, d_2^2 \cos^2\psi_2, d_3^2 \cos^2\psi_3, d_4^2 \cos^2\psi_4, d_1, d_2, d_3, d_4). \tag{23}$$

Similarly, jacobian matrices of non-redundant mechanism ($J_x^{Non-\mathrm{Red.}}$ and $J_q^{Non-\mathrm{Red.}}$) can be expressed as;

$$J_x^{Non-\mathrm{Red.}} = \begin{bmatrix} (\vec{s}_1 \times \overrightarrow{d_1})^T & (\vec{b}_1 \times (\vec{s}_1 \times \overrightarrow{d_1}))^T \\ (\vec{s}_2 \times \overrightarrow{d_2})^T & (\vec{b}_2 \times (\vec{s}_2 \times \overrightarrow{d_2}))^T \\ (\vec{s}_3 \times \overrightarrow{d_3})^T & (\vec{b}_3 \times (\vec{s}_3 \times \overrightarrow{d_3}))^T \\ \overrightarrow{d_1}^T & (\vec{b}_1 \times \overrightarrow{d_1})^T \\ \overrightarrow{d_2}^T & (\vec{b}_2 \times \overrightarrow{d_2})^T \\ \overrightarrow{d_3}^T & (\vec{b}_3 \times \overrightarrow{d_3})^T \end{bmatrix}, \tag{24}$$

and

$$J_q^{Non-\mathrm{Red.}} = diag(d_1^2 \cos^2\psi_1, d_2^2 \cos^2\psi_2, d_3^2 \cos^2\psi_3, d_1, d_2, d_3). \tag{25}$$

And for the Stewart platform one can have

$$J_x^{Stewart} = \begin{bmatrix} \overrightarrow{d_1}^T & (\vec{b}_1 \times \overrightarrow{d_1})^T \\ \overrightarrow{d_2}^T & (\vec{b}_2 \times \overrightarrow{d_2})^T \\ \overrightarrow{d_3}^T & (\vec{b}_3 \times \overrightarrow{d_3})^T \\ \overrightarrow{d_4}^T & (\vec{b}_4 \times \overrightarrow{d_4})^T \\ \overrightarrow{d_5}^T & (\vec{b}_5 \times \overrightarrow{d_5})^T \\ \overrightarrow{d_6}^T & (\vec{b}_6 \times \overrightarrow{d_6})^T \end{bmatrix}, \tag{26}$$

and

$$J_q^{Stewart} = diag(d_1, d_2, d_3, d_4, d_5, d_6). \tag{27}$$

Note that the joint velocity vector in stewart mechanism, $\dot{\bar{q}}^{Stewart}$, is the following 6×1 vector:

$$\dot{\bar{q}}^{Stewart} = [\dot{d}_1 \quad \dot{d}_2 \quad \dot{d}_3 \quad \dot{d}_4 \quad \dot{d}_5 \quad \dot{d}_6]^T . \tag{28}$$

Based on the existence of the two jacobian matrices above, the mechanism is at a singular configuration when either the determinant of J_x or J_q is either zero or infinity (Beji & Pascal, 1999).
Inverse kinematic singularity occurs when the determinant of J_q vanishes, namely;

$$\det(J_q) = 0 . \tag{29}$$

As it is clear from (25) and (27), the determinant of J_q in the workspace of this mechanism cannot be vanished. Therefore we do not have this type of singularity.
Forward kinematic singularity occurs when the rank of J_x is less than 6, namely;

$$rank(J_x) \leq 5 . \tag{30}$$

If (30) holds, the moving platform gains 1 or more degrees of freedom. In other words, at a forward kinematic singular configuration, the manipulator cannot resist forces or moments in some directions. As it can be seen, the redundancy can help us to avoid this kind of singularity, which is common in nearly all parallel mechanisms.

5. Performance indices

With the increasing demand for precise manipulators, search for a new manipulator with better performance has been intensive. Several indices have been proposed to evaluate the performance of a manipulator. Merlet reviewed the merits and weaknesses of these indices (Merlet, 2006). The dexterity indices have been commonly used in determining the dexterous regions of a manipulator workspace. The condition number of the jacobian matrix is known to be used as a measuring criterion of kinematic accuracy of manipulators. Salisbury & Craig (1982) used this criterion for the determination of the optimal dimensions for the fingers of an articulated hand. The condition number of the jacobian matrix has also been applied for designing a spatial manipulator (Angeles & Rojas, 1987).
The most performance indices are pose-dependant. For design, optimization and comparison purpose, Gosselin & Angeles (1991) proposed a global performance index, which is the integration of the local index over the workspace.
The performance indices are usually formed based on the evaluation of the determinant, norms, singular values and eigenvalues of the jacobian matrix. These indices have physical interpretation and useful application for control and optimization just when the elements of the jacobian matrix have the same units (Kucuk & Bingul, 2006). Otherwise, the stability of control systems, which are formed based on these jacobian matrices, will depend on the physical units of parameters chosen (Schwartz et al., 2002). Thus, different indices for rotations and translations should be defined (Cardou et al., 2010).

5.1 Manipulability

For evaluation of kinematic transmissibility of a manipulator, Yoshikawa (1984) defined the manipulator index,

$$\mu = \sqrt{\det(J^T J)} \,. \tag{31}$$

The manipulability can geometrically be interpreted as the volume of the ellipsoid obtained by mapping a unit n-dimensional sphere of joint space onto the Cartesian space (Cardou et al., 2010). It also can be interpreted as a measure of manipulator capability for transmitting a certain velocity to its end-effector (Mansouri & Ouali, 2011). To have a better performance for a manipulator, It is more suitable to have isotropic manipulability ellipsoid (Angeles & Lopez-Cajun, 1992). The isotropy index for manipulability can be defined as:

$$\mu_{iso} = \frac{\sigma_{Min}}{\sigma_{Max}} \,, \tag{32}$$

where σ_{Max} and σ_{Min} are maximum and minimum of singular values of jacobian matrix (J), respectively. The isotropy index is limited between 0 and 1. When the isotropy index is equal to 1, it indicates the ability of manipulator to transmit velocity uniformly from actuators to the end-effector along all directions. Inversely, when the isotropy index is equal to zero, the manipulator is at a singular configuration and cannot transmit velocity to the end-effector.

5.2 Dexterity

The accuracy of a mechanism is dependent on the condition number of the jacobian matrix, which is defined as follows:

$$k = \| J \| . \| J^{-1} \| \,, \tag{33}$$

where J is the jacobian matrix and $\|J\|$ denotes the norm of it and is defined as follows:

$$\| J \| = \sqrt{tr(\frac{1}{n} J J^T)} \,, \tag{34}$$

where n is the dimension of the square matrix J that is 3 for the manipulator under study. Gosselin (1992) defined the local dexterity (υ) as a criterion for measuring the kinematics accuracy of a manipulator,

$$\upsilon = \frac{1}{\| J \| . \| J^{-1} \|} \,. \tag{35}$$

The local dexterity can be changed between zero and one. The higher values indicate more accurate motion generated at given instance. When the local dexterity is equal to one, it denotes that the manipulator is isotropic at the given pose. Otherwise, it implies that the manipulator has reached a singular configuration pose.

To evaluate the dexterity of a manipulator over the entire workspace (W Gosselin & Angeles (1991) have introduced the global dexterity index (GDI) as:

$$GDI = \frac{\int_W \upsilon \; dW}{\int_W dW}, \tag{36}$$

which is the average value of local dexterity over the workspace. This global dexterity index can be used as design factor for the optimal design of manipulators (Bai, 2010; Li et al., 2010; Liu et al., 2010; Unal et al., 2008). Having a uniform dexterity is a desirable goal for almost all robotic systems. Uniformity of dexterity can be defined as another global performance index. It can be defined as the ratio of the minimum and maximum values of the dexterity index over the entire workspace,

$$\upsilon_{iso} = \frac{\upsilon_{Min}}{\upsilon_{Max}}. \tag{37}$$

5.3 Sensitivity

Evaluating of the kinematic sensitivity is another desirable concept in the performance analysis of a manipulator. The kinematic sensitivity of a manipulator can be interpreted as the effect of actuator displacements on the displacement of the end-effector. Cardou et al. (2010) defined two indices (τ_r , τ_p) for measuring the rotation and displacement sensitivity of a manipulator. They assumed the maximum-magnitude rotation and the displacement of the end-effector under a unit-norm actuator displacement as indices for calculating the sensitivity of a manipulator. The sensitivity indices can be defined as:

$$\tau_r = ||J_r||, \tag{38}$$

and

$$\tau_p = ||J_p||, \tag{39}$$

where J_r and J_p are rotation and translation jacobian martices (Cardou et al., 2010), respectively, where $||\ ||$ stands for a *p*-norm of the matrix. Cardou et al. (2010) suggested to use 2-norm and ∞-norm for calculating the sensitivity.

6. Comparison between 4-legged mechanism and other mechanisms

In order to investigate the kinematic performance of 4-legged mechanism, the response of the mechanisms are compared in several different aspects; reachable points, performance indices, and singularity analysis.

6.1 Reachable points and workspace comparison

Consider the 3-legged and the 4-legged mechanisms with g=1 m and h=0.5 m, respectively; g and h are the radii of the fixed and moving platforms, respectively.

By assuming a cubic with 1m length, 1 m width and 1 m height located 0.25 m above the base platform, we are interested in determining the reachability percentage in which each mechanism can successfully reach to the locations within this cubic space.

Table 1 shows that adding one leg to the 3-legged mechanism reduces the *R.P.* (Reachable points Percentage) by 5.03%. However, it should be noted that, although the non-redundant mechanism has a wider workspace, it has much more singular points than the redundant mechanism, and actuator forces and torques are also less in the redundant mechanism. As it can be seen from Table 1, *RP*s in the Stewart platforms are smaller than 3-legged and 4-legged mechanisms. In the 6-legged Stewart-like UPS mechanisms (Stewart, 1965), the workspace is constructed by intersecting of 6 spheres. On the other hand, in the proposed 4-legged UPS mechanism, the workspace is constructed by intersecting of only 4 spheres.

Mechanism	% RP
Stewart (6-6)	76.35
Stewart (3-6)	74.21
Stewart (6-3)	73.70
Stewart (3-3)	63.46
3-legged mechanism	84.75
4-legged mechanism	79.72

Table 1. Reachable points

Assuming similar dimensions for the two mechanisms result in a larger workspace for the 4-legged mechanism.
To compare the workspace of the proposed 4-legged mechanism with the 3-legged mechanism and Steward platforms, the reachable points for them were calculated and obtained results are shown in Fig. 6 It is appear that the 3-legged mechanism has the largest workspace followed by 4-legged mechanism, 3-6 and 3-3 Steward Platforms.

6.2 Performance comparison

To compare the kinematic performance of the proposed 4-legged mechanism with the 3-legged mechanism and Steward platform, abovementioned performance indices were used. The results obtained are shown in Figs. 7 to 10. These figures show how performance indices vary on a plate ($Z=0.75$) within the workspace.
Fig. 7 depicts the Stewart 3-3 has the higher isotropy index for manipulability comparing with Stewart 3-6, 3-legged and 4-legged mechanisms. After Stewart 3-3, the 4-legged mechanism presents the better performance. This figure illustrates that adding a leg to a 3-legged mechanism can significantly improve the manipulability of the mechanism. Furthermore, a 4-legged mechanism can have a performance comparable with the Stewart platforms or even better.
Fig. 8 depicts the Stewart 3-3 compared with the other mechanisms under study has the higher dexterity index. After Stewart 3-3, again, the 4-legged mechanism presents the better performance. This figure also illustrates significant enhancement of the dexterity of the mechanism due to the additional leg. Also it shows that, in terms of dexterity, the 4-legged mechanism can have a comparable performance against the Stewart platforms or even better.
In the next step of performance comparison of manipulators, displacement and rotation sensitivities for mechanisms of our interest are compared. Fig. 9 shows the amount of displacement sensitivity indices of the abovementioned mechanisms on the selected plane

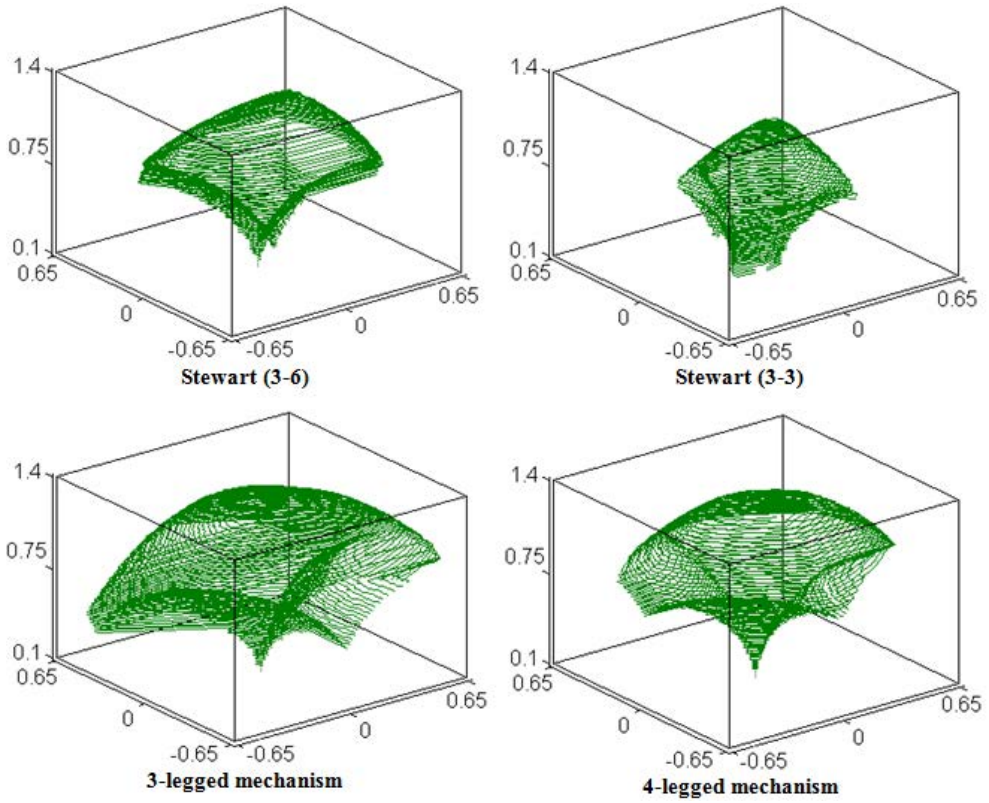

Fig. 6. Workspaces of Stewart (3-6), Stewart (3-3), 3-legged and 4-legged mechanisms.

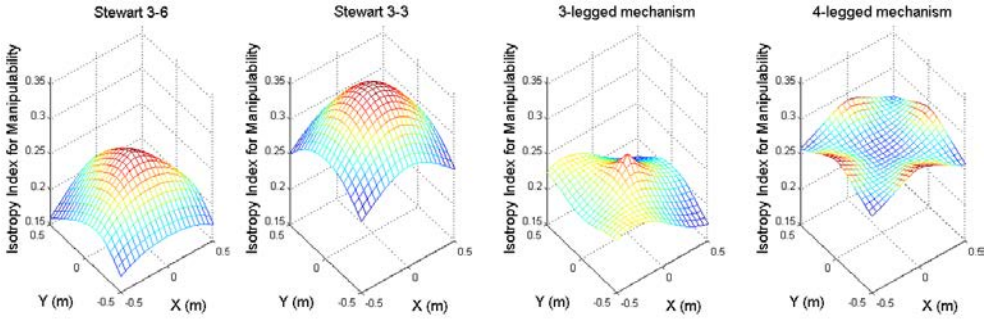

Fig. 7. Isotropy index for manipulability of Stewart 6-6, Stewart 3-6, 3 Legged mechanism and 4 legged mechanism on the plane z= 0.75 m

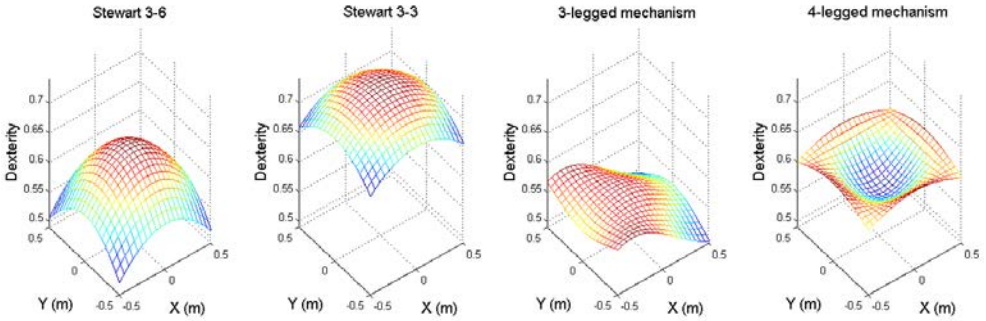

Fig. 8. Dexterity index of Stewart 6-6, Stewart 3-6, 3-Legged mechanism and 4-legged mechanism on the plane z= 0.75 m.

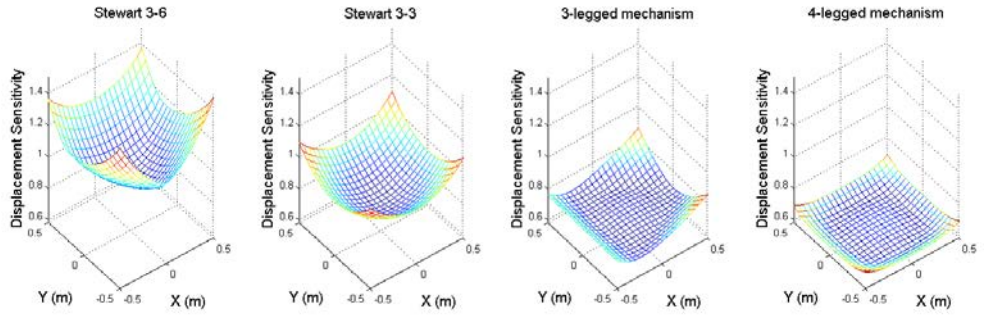

Fig. 9. Displacement Sensitivity index of Stewart 6-6, Stewart 3-6, 3-Legged mechanism and 4-legged mechanism on the plane z= 0.75 m.

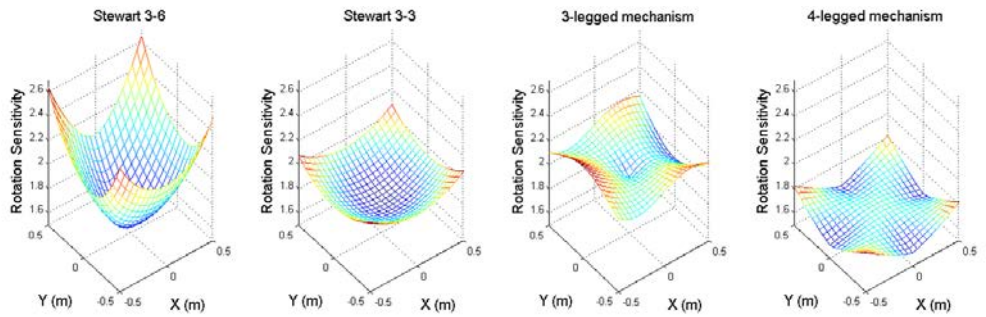

Fig. 10. Rotation Sensitivity index of Stewart 6-6, Stewart 3-6, 3-Legged mechanism and 4-legged mechanism on the plane z= 0.75 m.

($Z=0.75$). It clearly shows that the 4-legged mechanism has less displacement sensitivity index by far. Fig. 10 depicts the 4-legged mechanism has also less rotation sensitivity compared with other mechanisms.
So far from Figs. 7 to 10, the amounts of performance indices are shown on the planes. To compare the kinetics performance of manipulators over the entire workspace, the global performance Index (GPI) can be evalueated as:

$$GPI = \frac{\int_W PI \ \ dW}{\int_W dW}, \tag{40}$$

which is the average value of local performance index (PI) over the workspace (W).
The amounts of GPI for Isotropy Index for Manipulability (IIM), Dexterity (DX), Displacement Sensitivity (DS) and Rotation Sensitivity (RS) were calculated and obtained results were listed in Table 2.
Table 2 shows that the 4-legged mechanism has a better IIM within the selected workspace, which explicitly indicates a better ability for transmitting a certain velocity to its end-effector.
As it is seen from Table 2, the Stewart 3-3 platform has the biggest global DX compared with other mechanisms and the 4-legged mechanism has the second (i.e. difference in DX is only 5.71% less). It represents that the Stewart 3-3 platform and the proposed 4-legged mechanism have the better kinematics accuracy.
Having the lower sensitivity is a demand for industrial mechanisms. By comparing the values of DS and RS, which are listed in Table 2, it is obvious the 4-legged mechanism is an appropriate candidate.
Based on the results shown in Table 2, the 4-legged mechanism is recommended for better kinematic performances

	The higher, the better		The lower, the better	
Mechaniasm	*IIM*	*DX*	*DS*	*RS*
Stewart (6-6)	0.0429	0.1589	1.3249	3.5791
Stewart (3-6)	0.1296	0.3969	1.2070	2.5725
Stewart (6-3)	0.1020	0.3449	1.2113	2.8991
Stewart (3-3)	0.1978	**0.5284**	1.0485	2.6077
3-legged mechanism	0.1136	0.3423	0.8538	2.3861
4-legged mechanism	**0.2140**	0.4982	**0.7279**	**1.8441**

Table 2. Performance comparison between 3-legged mechanism, 4-legged mechanism, Stewart 6-6, and Stewart 3-6

6.3 Singularity analysis of 3-legged and 4-legged mechanisms

Several types of workspace can be considered. For example, the 3D constant orientation workspace, which describes all possible locations of an arbitrary point P in the moving system with a constant orientation of the moving platform, the reachable workspace (all the

locations that can be reached by P), the orientation workspace (all possible orientations of the end-effector around P for a given position) or the inclusive orientation workspace (all the locations that can be reached by the origin of the end-effector with every orientation in a given set) (Abedinnasab & Vossoughi, 2009).

Out of those types, we have used the inclusive orientation workspace, where for every position in a fixed surface, the moving platform is rotated in every possible orientation to determine if that configuration is singular or not. After trials and errors, we figured out that for a better determination of the singular configurations, the roll-pitch-yaw rotation about the global coordinate is the most critical set of rotations compared to the other rotations such as the reduced Euler rotations.

To illustrate the positive effects of redundancy on eliminating singular configurations, we have done jacobian analysis in planes in different orientations of the workspace as shown in Fig. 11. The results are shown in Figs. 12 and 13. In Figs. 12 and 13, the jacobian determinant of center of the moving platforms of 3-legged and 4-legged mechanisms has been calculated. The platform is rotated simultaneously in three different directions according to the roll-pitch-yaw Euler angles discussed above. Each angle is free to rotate up to ±20°. After the rotations in each position, if the mechanism did not encounter any singular configuration, the color of that position is represented by light gray. If there was any singular configuration inside ±20° region and beyond ±10° region, the color is dark gray. At last, if the singular configuration was encountered in ±10° rotations, the color is black.

As seen from Fig. 12, in the 3-legged mechanism, there exist singular configurations in the most of the X-Y, X-Z and Y-Z planes (black and dark gray regions). However, in the 4-legged mechanism, the singular points do not exist at the most of the plane. Figure 13 shows the same patterns as in the other planes. Figures 12 and 13 simply illustrate the great effect of a simple redundancy; namely, the addition of a leg to the 3-legged mechanism can remove vast singular configurations.

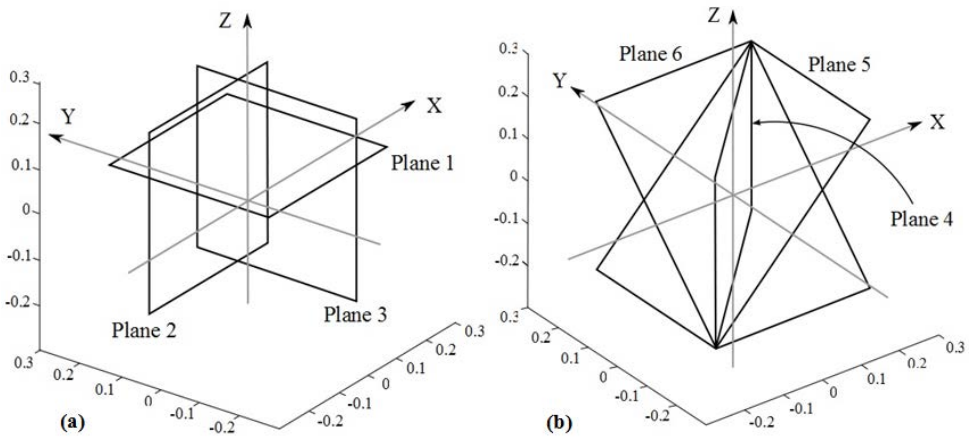

Fig. 11. (a) Schematic view of planes 1, 2, and 3. (b) Schematic view of planes 4, 5, and 6.

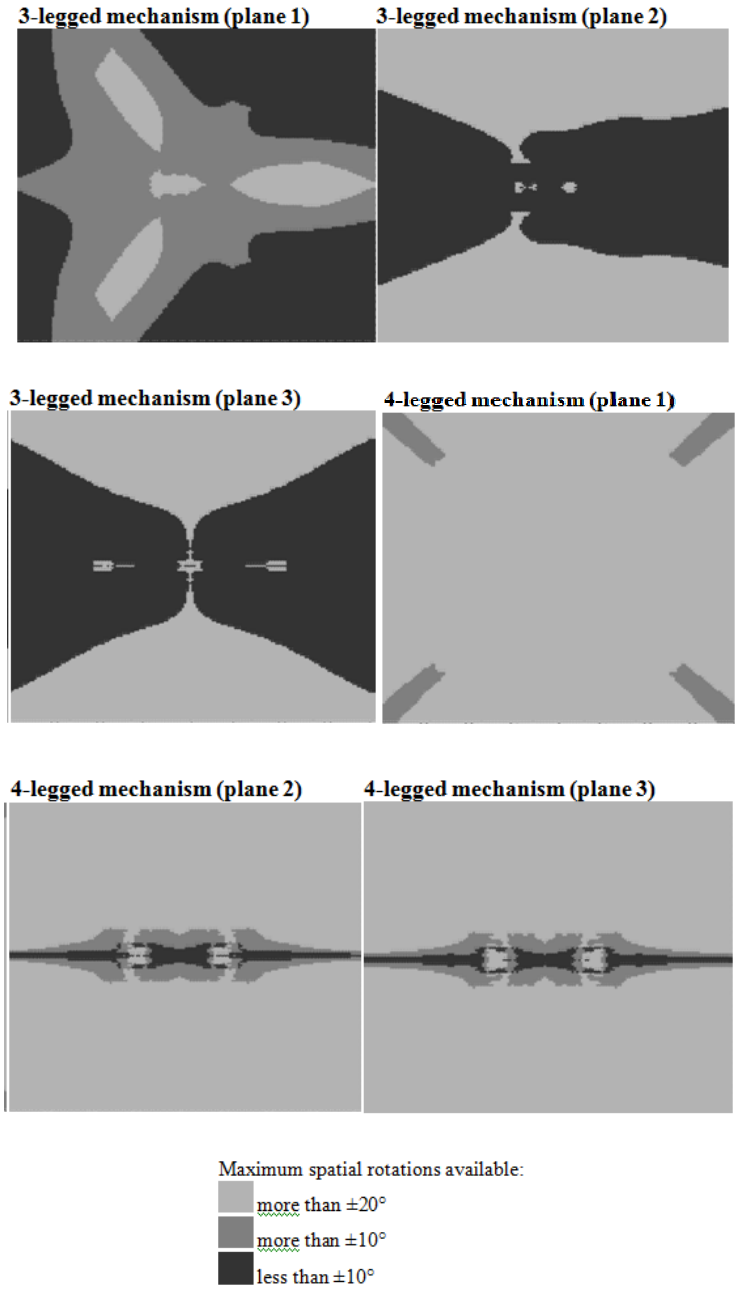

Fig. 12. Singularity analysis in planes 1, 2 and 3 for both 3-legged (non-redundant) and 4-legged (redundant) mechanisms.

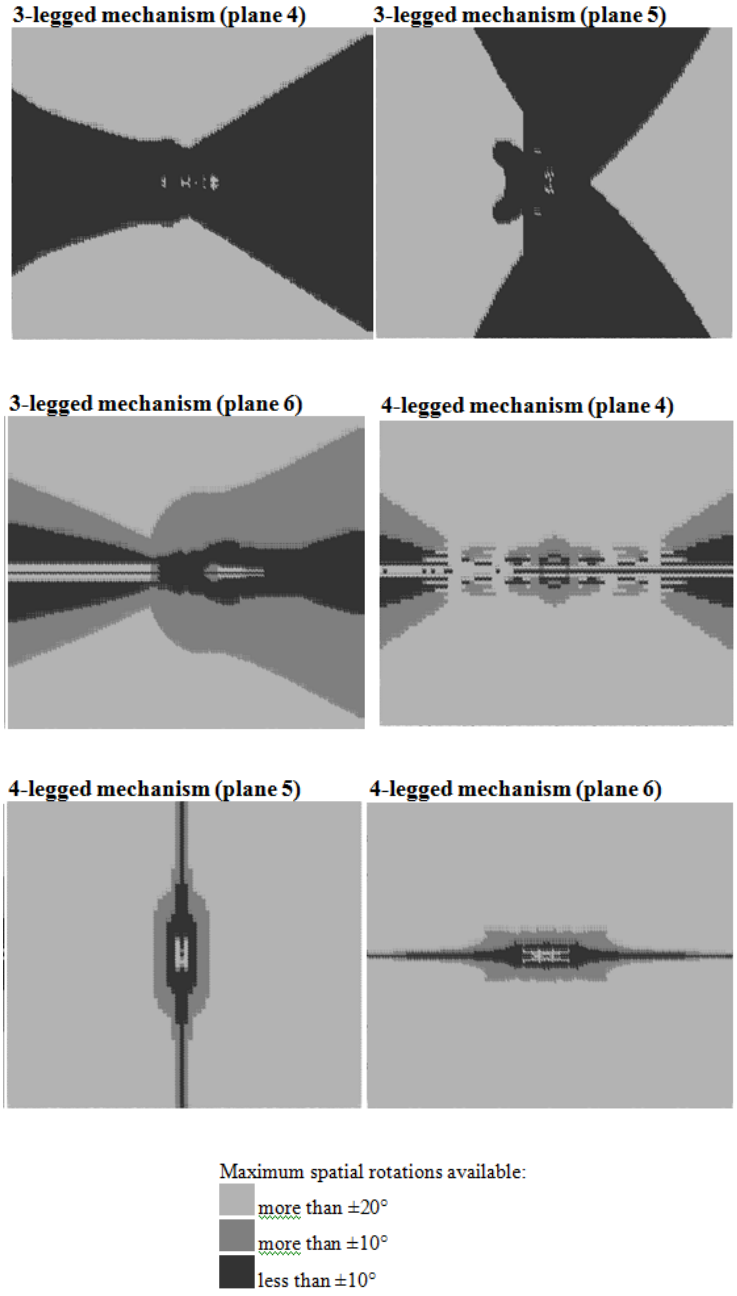

Fig. 13. Singularity analysis in planes 4, 5 and 6 for both 3-legged (non-redundant) and 4-legged (redundant) mechanisms.

7. Conclusion

The effects of redundant actuation are studied. The redundant 4-legged and non-redundant 3-legged parallel mechanisms are compared with 4 well-known architectures of Gough-Stewart platforms. It is shown that the inverse kinematics of the proposed 3-legged and 4-legged mechanisms have a closed-form solution. Also the Jacobian matrix has been determined using the concept of reciprocal screws.

From the design point of view, by replacing the passive universal joints in the Stewart platforms with active joints in the above mentioned mechanisms, the number of legs could be reduced from 6 to 3 or 4. It makes the mechanism to be lighter, since the rotary actuators are resting on the fixed platform, which allows higher accelerations to be available due to smaller inertial effects.

It is illustrated that redundancy improves the ability and performance of the non-redundant parallel manipulator. The redundancy brings some advantages for parallel manipulators such as avoiding kinematic singularities, increasing workspace, improving performance indices, such as dexterity, manipulability, and sensitivity. Finally, we conclude that the redundancy is a key choice to remove singular points, which are common in nearly all parallel mechanisms.

It is worthy to state that the applications of these robots can be found in flight simulators, high precision surgical tools, positioning devices, motion generators, ultra-fast pick-and-place robots, haptic devices, entertainment, multi-axis machine tools, micro manipulators, rehabilitation devices, etc.

8. References

Abedinnasab, M. H. & Vossoughi, G. R. (2009). Analysis of a 6-dof redundantly actuated 4-legged parallel mechanism, Nonlinear Dyn. 58(4): 611–622.

Aghababai, O. (2005). Design, Kinematic and Dynamic Analysis and Optimization of a 6 DOF Redundantly Actuated Parallel Mechanism for Use in Haptic Systems, MSc Thesis, Sharif University of Technology, Tehran, Iran.

Alp, H. & Özkol, I. (2008). Extending the workspace of parallel working mechanisms, Proc. Inst. Mech. Eng., Part C: J. Mech. Eng. Sci. 222(7): 1305–1313.

Angeles, J. & Lopez-Cajun, C. S. (1992). Kinematic isotropy and the conditioning index of serial robotic manipulators, Int. J. Rob. Res. 11(6): 560–571.

Angeles, J. & Rojas, A. A. (1987). Manipulator inverse kinematics via condition-number minimization and continuation, Int. J. Rob. Autom. 2: 61–69.

Arata, J., Kondo, J., Ikedo, N. & Fujimoto, H. (2011). Haptic device using a newly developed redundant parallel mechanism, IEEE Trans. Rob. 27(2): 201–214.

Bai, S. (2010). Optimum design of spherical parallel manipulators for a prescribed workspace, Mech. Mach. Theory 45(2): 200–211.

Beji, L. & Pascal, M. (1999). Kinematics and the full minimal dynamic model of a 6-dof parallel robot manipulator, Nonlinear Dyn. 18: 339–356.

Cardou, P., Bouchard, S. & Gosselin, C. (2010). Kinematic-sensitivity indices for dimensionally nonhomogeneous jacobian matrices, IEEE Trans. Rob. 26(1): 166–173.

Choi, H. B., Konno, A. & Uchiyama, M. (2010). Design, implementation, and performance evaluation of a 4-DOF parallel robot, Robotica 28(1): 107–118.

Deidda, R., Mariani, A. & Ruggiu, M. (2010). On the kinematics of the 3-RRUR spherical parallel manipulator, Robotica 28(6): 821–832.

Gallardo-Alvarado, J., Aguilar-Nájera, C. R., Casique-Rosas, L., Rico-Martínez, J. M. & Islam, M. N. (2008). Kinematics and dynamics of 2(3-RPS) manipulators by means of screw theory and the principle of virtual work, Mech. Mach. Theory 43(10): 1281–1294.

Gallardo-Alvarado, J., Orozco-Mendoza, H. & Rico-Martínez, J. M. (2010). A novel five-degrees-of-freedom decoupled robot, Robotica 28(6): 909–917.

Gallardo-Alvarado, J., Rico-Martínez, J. M. & Alici, G. (2006). Kinematics and singularity analyses of a 4-dof parallel manipulator using screw theory, Mech. Mach. Theory 41(9): 1048–1061.

Gan, D., Liao, Q., Dai, J. & Wei, S. (2010). Design and kinematics analysis of a new 3CCC parallel mechanism, Robotica 28: 1065–1072.

Gao, Z., Zhang, D., Hu, X. & Ge, Y. (2010). Design, analysis, and stiffness optimization of a three degree of freedom parallel manipulator, Robotica 28(3): 349–357.

Gosselin, C. & Angeles, J. (1990). Singularity analysis of closed-loop kinematic chains, IEEE Trans. Rob. Autom. 6(3): 281–290.

Gosselin, C. & Angeles, J. (1991). Global performance index for the kinematic optimization of robotic manipulators, J. Mech. Transm. Autom. Des. 113(3): 220–226.

Gosselin, C. M. (1992). The optimum design of robotic manipulators using dexterity indices, Rob. Autom. Syst. 9(4): 213–226.

Gough, V. E. & Whitehall, S. G. (1962). Universal tyre test machine, in Proc 9th Int. Tech. Congress FISITA pp. 117–137.

Jiang, Q. & Gosselin, C. M. (2009a). Determination of the maximal singularity-free orientation workspace for the gough-stewart platform, Mech. Mach. Theory 44(6): 1281–1293.

Jiang, Q. & Gosselin, C. M. (2009b). Evaluation and Representation of the Theoretical Orientation Workspace of the Gough-Stewart Platform, J. Mech. Rob., Trans. ASME 1(2): 1–9.

Jiang, Q. & Gosselin, C. M. (2009c). Maximal Singularity-Free Total Orientation Workspace of the Gough-Stewart Platform, J. Mech. Rob., Trans. ASME 1(3): 1–4.

Kucuk, S. & Bingul, Z. (2006). Comparative study of performance indices for fundamental robot manipulators, Rob. Autom. Syst. 54(7): 567–573.

Li, H., Gosselin, C. M. & Richard, M. J. (2007). Determination of the maximal singularity-free zones in the six-dimensional workspace of the general, Mech. Mach. Theory 42(4): 497–511.

Li, J.,Wang, S.,Wang, X. & He, C. (2010). Optimization of a novel mechanism for a minimally invasive surgery robot, Int. J. Med. Rob. Comput. Assisted Surg. 6(1): 83–90.

Liu, X., Xie, F., Wang, L. & Wang, J. (2010). Optimal design and development of a decoupled A/B-axis tool head with parallel kinematics, Adv. Mech. Eng. 2010: 1–14.

Lopes, A. M. (2010). Complete dynamic modelling of a moving base 6-dof parallel manipulator, Robotica 28(5): 781–793.

Lu, Y., Hu, B., Li, S.-H. & Tian, X. B. (2008). Kinematics/statics analysis of a novel 2SPS + PRRPR parallel manipulator, Mech. Mach. Theory 43(9): 1099–1111.

Lu, Y., Hu, B. & Yu, J. (2009). Analysis of kinematicsstatics and workspace of a 2(SP+SPR+SPU) serial-parallel manipulator, Multibody Sys. Dyn. 21(4): 361–374.

Lu, Y., Shi, Y. & Yu, J. (2010). Determination of singularities of some 4-dof parallel manipulators by translational/rotational jacobian matrices, Robotica 28(6): 811–819.

Mansouri, I. & Ouali, M. (2011). The power manipulability a new homogeneous performance index of robot manipulators, Rob. Comput. Integr. Manuf. 27(2): 434–449.

Masouleh, M. T., Gosselin, C., Husty, M. & Walter, D. R. (2011). Forward kinematic problem of 5-RPUR parallel mechanisms (3T2R) with identical limb structures, Mech. Mach. Theory 46(7): 945–959.

Merlet, J. P. (2006). Jacobian, manipulability, condition number, and accuracy of parallel robots, J. Mech. Des., Trans. ASME 128(1): 199–206.

Müller, A. (2005). Internal preload control of redundantly actuated parallel manipulators – its application to backlash avoiding control, IEEE Trans. Rob. 21(4): 668–677.

Pendar, H., Mahnama, M. & Zohoor, H. (2011). Singularity analysis of parallel manipulators using constraint plane method, Mech. Mach. Theory 46(1): 33–43.

Piipponen, S. (2009). Singularity analysis of planar linkages, Multibody Sys. Dyn. 22(3): 223–243.

Ropponen, T. & Nakamura, Y. (1990). Singularity-free parameterization and performance analysis of actuation redundancy, Proc. IEEE Int. Conf. Robot. Autom. 2: 806–811.

Sadjadian, H. & Taghirad, H. D. (2006). Kinematic, singularity and stiffness analysis of the hydraulic shoulder: A 3-dof redundant parallel manipulator, Adv. Rob. 20(7): 763–781.

Salisbury, J. K. & Craig, J. J. (1982). Articulated hands - force control and kinematic issues, Int. J. Rob. Res. 1(1): 4–17.

Schwartz, E., Manseur, R. & Doty, K. (2002). Noncommensurate systems in robotics, Int. J. Rob. Autom. 17(2): 86–92.

St-Onge, B. M. & Gosselin, C. M. (2000). Singularity analysis and representation of the general gough-stewart platform, Int. J. Rob. Res. 19(3): 271–288.

Staicu, S. (2009). Dynamics of the spherical 3-U-PS/S parallel mechanism with prismatic actuators, Multibody Sys. Dyn. 22(2): 115–132.

Stewart, D. (1965). A platform with six degrees of freedom, Proc. Inst. Mech. Eng. 180: 371–386.

Tsai, L.-W. (1998). The jacobian analysis of a parallel manipulator using reciprocal screws in Advances in Robot Kinematics: Analysis and Control, J. Lenarcic and M. L. Husty, Eds., Kluwer Academic.

Tsai, L.-W. (1999). Robot analysis: the mechanics of serial and parallel manipulators, Wiley.

Unal, R., Kizltas, G. & Patoglu, V. (2008). A multi-criteria design optimization framework for haptic interfaces, Symp. Haptic Interfaces Virtual Environ. Teleoperator Syst. pp. 231–238.

Vischer, P. & Clavel, R. (1998). Kinematic calibration of the parallel delta robot, Robotica 16(2): 207–218.

Wang, J. & Gosselin, C. M. (2004). Kinematic analysis and design of kinematically redundant parallel mechanisms, J. Mech. Des., Trans. ASME 126(1): 109–118.

Wu, J., Wang, J. & wang, L. (2010). A comparison study of two planar 2-DOF parallel mechanisms : one with 2-RRR and the other with 3-RRR structures, Robotica 28(6): 937–942.

Yi, B.-J., Freeman, R. A. & Tesar, D. (1989). Open-loop stiffness control of overconstrained mechanisms/robotic linkage systems, Proc. IEEE Int. Conf. Robot. Autom. 3: 1340 – 1345.

Yoshikawa, T. (1984). Analysis and control of robot manipulators with redundancy, Int. Symp. Rob. Res. pp. 735–747.

Zhao, J., Feng, Z., Zhou, K. & Dong, J. (2005). Analysis of the singularity of spatial parallel manipulator with terminal constraints, Mech. Mach. Theory 40(3): 275–284.

Zhao, Y. & Gao, F. (2010). The joint velocity, torque, and power capability evaluation of a redundant parallel manipulator. accepted in Robotica.

Zhao, Y., Liu, J. F. & Huang, Z. (2011). A force analysis of a 3-rps parallel mechanism by using screw theory. accepted in Robotica.